Effect of molecular weight on drawing poly(vinyl alcohol) from solution-grown crystal mats

Tetsuo Kanamoto*, Sumito Kiyooka and Yurii Tovmasyan†
Department of Applied Chemistry, Science University of Tokyo, Kagurazaka, Shinjuku-ku, Tokyo 162, Japan

and Hirofumi Sano and Hiroshi Narukawa
Kuraray Co. Ltd, Sakazu, Kurashiki, Okayama 710, Japan
(Received 2 October 1989; revised 6 November 1989; accepted 16 November 1989)

Solution-grown crystal (SGC) mats of poly(vinyl alcohol) (PVA) with different degrees of polymerization ($DP = 3500$–$18\,200$), precipitated from dilute solutions in ethylene glycol, were drawn by solid state coextrusion followed by tensile drawing at elevated temperatures (two-stage drawing). The SGC mats exhibited significant strain hardening during the second-stage tensile drawing. The draw stress at a given draw ratio (DR) was higher for higher DP samples. Although the draw stress decreased and the maximum achievable DR increased with increasing drawing temperature, the practically highest temperature was limited to $\leqslant 220$°C, due to thermal degradation at higher temperatures. The maximum DR thus achieved at 220°C, as well as the efficiency of draw evaluated by the thermal elastic shrinkage, was not significantly affected by the sample DP in the range studied in this work. The ambient tensile modulus and strength increased rapidly with DR up to 50 and 1.3 GPa, respectively, at the highest achieved DR of 20 for each DP, showing no significant effect of sample DP on either the drawability or the resultant tensile properties of drawn films. Thus, among several properties examined, only the draw and fracture stresses at elevated temperatures and the differential scanning calorimetry melting temperature of drawn samples were significantly affected by DP, being markedly higher for higher DP samples. These features in drawing SGC mats of PVA are markedly different from those previously observed in superdrawing of SGC mats of polyethylenes with different molecular weights.

(Keywords: drawing; poly(vinyl alcohol); effect of molecular weight; tensile properties; physical properties)

INTRODUCTION

Ultradrawing of semicrystalline polymers has been the subject of intensive studies with the goal of achieving the limiting chain extension and orientation which may lead to the maximum mechanical and physical properties[1–3]. The most extensively studied polymer has been high density polyethylene (PE). For this, it has been established that the tensile modulus and strength steadily increase with draw ratio (DR). The most successful ultradraw has been achieved for ultrahigh molecular weight PE (UHMW-PE), by flow induced crystallization from solutions[4] and tensile drawing of gel[5–7] and single crystal (SGC) mats[8,9] prepared from semi-dilute and dilute solutions, respectively. The dramatically improved ductility ($DR \leqslant 350$) for these solution-grown crystal morphologies, in comparison to melt-crystallized forms ($DR \leqslant 10$), has been explained in terms of the reduced number of entanglements[10] and/or the regularity of chain folding[11] for the former. We have found that the drawability and efficiency of draw for SGC mats of UHMW-PE also depend significantly on the techniques used[12,13] and the sample MW[14]. Among several techniques examined, solid state coextrusion, developed by Griswold *et al.*[15], followed by tensile drawing (two-stage drawing) gave the most efficient and highest draw[12–14]. The superdrawn films exhibited tensile moduli of $\leqslant 220$–230 GPa and strengths of $\leqslant 4$–5.5 GPa at $DR \geqslant 250$, the former approaching the X-ray crystal modulus reported for a crystal of PE (235 GPa)[16].

More recently, poly(vinyl alcohol) (PVA) has become a second candidate for producing a high modulus, high strength material by ultradrawing, since this polymer has theoretically high mechanical properties[16,17] comparable with those of PE. Another advantage of PVA is its high melting temperature (≈ 240°C) compared to PE (≈ 140°C). Grubb *et al.* have studied drawing of PVA gel by tensile drawing[18] and zone drawing[19]. They reported that the maximum achievable DR (DR_{max}) for dry gel was ≈ 15 for both techniques, and it increased markedly up to 37 with zone drawing of plasticized gels with ethylene glycol (EG). However, the resultant drawn films from wet gel had significantly higher void fractions than those drawn without the solvent, and had lower tensile strength. Kwon *et al.*[20] obtained high modulus ($\leqslant 64$ GPa) and strength ($\leqslant 2.3$ GPa) fibres by gel spinning/drawing of UHMW-PVA; even the DR of such fibres were low ($\leqslant 10$). Hyon *et al.*[21] found that the properties of PVA gels, including ductility, depend markedly on the solvent systems from which gels were generated.

* To whom correspondence should be addressed
† On leave from The Institute of Chemical Physics, USSR Academy of Sciences, Kosygin Str., 4, Moscow 117977, USSR

0032-3861/90/112039-08

We have also studied drawing of PVA based on knowledge obtained from previous success in superdrawing of UHMW-PE[12–14]. In this paper, the effect of MW on drawing SGC mats of PVA is reported. Some of the results are compared with those previously observed in superdrawing of SGC mats of PE with a range of MW, 2×10^5–80×10^5.

EXPERIMENTAL

Samples

The three atactic PVA samples used had degrees of polymerization (DP) of 3500, 7700 and 18 200, respectively, and were highly saponified (>99.8%). Solution-grown crystals (SGC) of PVA were isothermally precipitated from 0.1 wt% (0.085 vol%) solutions in ethylene glycol (EG) kept at 50°C for 20 h. To minimize the oxidative degradation during dissolution and crystallization, a mixture of the requisite amounts of PVA powder and EG solvent was placed in a 500 ml Kielder flask and degassed under vacuum. After repeating the freezing by liquid nitrogen and melting cycle under vacuum three times to completely remove the dissolved air, the flask was sealed off. The mixture in a flask was heated in a silicone oil bath up to 150–170°C, with slow stirring by a magnetic stirrer, and held there for 0.5–3 h, depending on the sample DP, to obtain a homogeneous solution. The flask containing a hot solution was transferred to a silicone oil bath at 50°C and kept there for 20 h to consolidate precipitation. SGC mats were obtained by filtering the crystal suspension at room temperature. A small amount of EG remaining in the mat was completely removed by extracting with boiling methanol in a Soxhlet apparatus for 10 h, followed by drying in *vacuo at* 40°C.

Drawing

A two-stage drawing technique[12,13] was used for drawing SGC mats of PVA. For the first-stage drawing, the solid state coextrusion technique[15] was used. One or two mats were placed between split billet halves of poly(4-methyl-1-pentene) and the assembly coextruded at a constant temperature of 160°C and at low extrusion draw ratios (EDR) of 3–6. For the second-stage, the extrudates were drawn by tensile force in an air oven equipped with a Tensilon tensile tester at 220°C and at constant cross-head speeds, which gave an initial strain rate of $5\,min^{-1}$.

Characterization

The tensile modulus and strength on the fibre axis were measured at room temperature and at strain rates of 1×10^{-3} and $1 \times 10^{-2}\,s^{-1}$, respectively. The modulus was determined from the slope of the stress–strain curve at low strain (<0.1%). The sample lengths for the measurements of modulus and strength were ≈25 and 5 cm, respectively.

Melting behaviour of drawn films was measured on a Seiko–Denshi DSC-10 at a heating rate of $3°C\,min^{-1}$. Melting temperatures and heats of fusion were calibrated with an Indium standard. The sample sizes were 0.05 and 0.5 mg for determination of melting peak temperatures and heats of fusion, respectively.

Wide-angle (WAXD) and small-angle (SAXS) X-ray scattering patterns were recorded by flat plate cameras with Ni-filtered CuKα radiation generated by a Rigaku RU-200 rotating anode generator with a fine focus cathode operated at 40 kV and 25 mA. The sample to film distances were 40 and 250 (400) mm for WAXD and SAXS, respectively. The exposure times for SAXS were 20–60 h depending on the DR of samples.

Thermally induced elastic shrinkage was measured by quickly immersing a drawn sample, 1 cm in length, in a silicone oil bath kept at 270°C for 15 s.

RESULTS AND DISCUSSION

The ductility of SGC mats of PVA increased significantly with increasing drawing temperature. However, PVA was unstable at high temperatures approaching the melting point (240°C). When PVA was heated to ≥230°C for several minutes in air, a marked degradation occurred, as indicated by the dark brown colour of the sample. Thus the first-stage, solid-state coextrusion was performed at 160°C, where apparently no degradation occurred during extrusion. The second-stage tensile drawing of the coextrudates was made at 220°C, where extensive degradation could be suppressed, as shown by a faint colour for the resultant drawn materials.

Drawing behaviour

Figure 1 shows nominal draw stress *versus* strain curves for the second-stage tensile drawing of initial EDR 3 extrudates prepared from PVA with DP=3500, 7700 and 18 200. The curves were recorded at 220°C and a constant cross-head speed, giving an initial extension rate of $5\,min^{-1}$. Only a low strain region (≤3) is shown, since the relations between stress and strain at higher strains were obscured due to the frequent occurrence of sample slippage at the cramp during drawing. Marked effects of sample DP are seen on these curves. The yield stress at a strain of 0.20–0.25 was slightly higher for higher DP

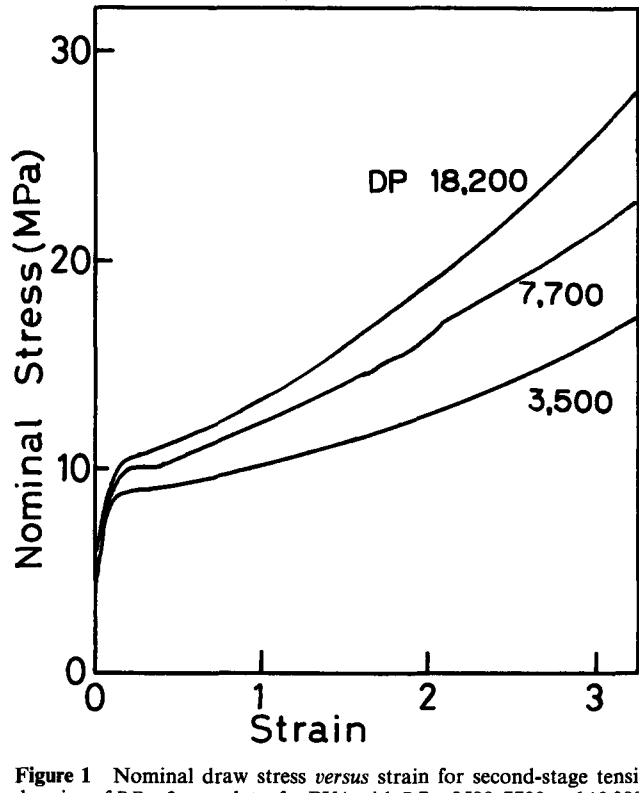

Figure 1 Nominal draw stress *versus* strain for second-stage tensile drawing of DR = 3 extrudates for PVA with DP = 3500, 7700 and 18 200

samples. After yielding, the nominal stresses increased steadily as the samples were elongated. Such strain hardening was more prominent for higher *DP* samples and most of the test samples fractured at a comparable strain of 5–6 (corresponding to $DR = 18$–21). Thus the nominal fracture stress for the second-stage drawing at 220°C increased with sample *DP*. The tensile strengths at this high temperature, estimated by dividing the nominal fracture stress by the cross-sectional area, increased with the sample *DP* and were 145–170, 180–210 and 240–280 MPa for $DP = 3500$, 7700 and 18 200, respectively. However, the maximum *DR* achieved for SGC mats was independent of sample *DP* and ≈ 20 in this work, due to the higher draw stress for higher *DP* samples. Such a higher draw stress and fracture stress for a higher *DP* sample are consistent with the expectation that the number of net points for a molecule, formed by the incorporation of the molecular segments in crystallites or by the entanglements, may increase with increasing molecular chain length (or *DP*), resulting in an enhanced morphological continuity. The maximum *DR* attained here is slightly higher than that ($DR = 15$) reported from tensile drawing of plasticized gel[18] of a lower *DP* (≈ 2000) and that ($DR = 10$) which appeared in a patent claim[20] for gel spinning/drawing of high molecular weight PVA samples ($DP = 10\,000$–$40\,000$). However, this *DR* is markedly lower than those achieved by tensile drawing of the gel prepared from a solution in a mixed solvent consisting of DMSO/H_2O = 4/1[21], and by zone drawing of a partially plasticized gel with EG (DR_{max} of 15 for dry gel *versus* 37 for wet gel)[19]. Remember that the resultant fibres from the wet gel had significantly higher void fractions than those drawn without EG, and had lower tensile strength[19].

The drawing behaviour of PVA is strikingly different from that observed in superdrawing of polyethylene (PE)[12–14]. The drawability of the latter was dramatically affected by both the sample *MW* and the initial morphology. The maximum *DR* achieved for a melt crystallized spherulitic form of PE decreased with increasing sample *MW* from 35 for normal MW-PE to 10 for UHMW-PE[1,2]. However, UHMW-PE has been shown to be ultradrawable up to $DR = 130$–350 by drawing from SGC mats[8,9,12–14] and gels[3,5–7], which were prepared from dilute and semidilute solutions, respectively. Such a dramatic increase in the ductility for these morphologies has been explained on the basis of the chain entanglement concept proposed by Smith *et al.*[10]. Even for PVA, the entanglement density or the segmental counter length between the neighbouring entanglements may also be one of the important parameters determining the ductility of samples. This may be determined by the solution concentration and mode of solidification from solutions.

Narukawa *et al.*[22,23] have studied the rheological properties of PVA solutions in DMSO. They determined the critical polymer concentrations C^* and C_e as a function of *DP*. C^* corresponds to the critical concentration above which the molecules in solution overlap, whereas C_e is that above which intermolecular chain entanglements are formed. Thus, a coherent gel is not formed from a solution with concentration below C^*. As EG used here is as good a solvent as DMSO for PVA, a rough estimate of these critical concentrations may be made based on their data, and is shown in *Table 1*. This is further supported by the observation that no coherent gel was formed from 0.1 wt% (0.085 vol%) solutions in EG for the range of sample *DP* used in this work. Thus, if crystallization proceeds directly from dilute solutions, as will be discussed later, the number of trapped entanglements in SGC mats may be nil for all *DP* samples. Kanamoto and Porter[24] analysed the deformation of UHMW-PE SGC mats based on the models combining the effect of molecular weight, initial molecular state and deformation mode. They found that the minimum draw ratio (DR_{min}) necessary for full chain extension from a random coil in θ dimension is close to the actual superdraw process. According to this model, DR_{min} for a linear polymer[3] is given by

$$DR_{min} = L/\langle r_0 \rangle^{1/2} = 0.83(n/C_\infty)^{1/2}$$

where L is the molecular chain length, $\langle r_0 \rangle^{1/2}$ the mean square end to end distance, n the number of skeletal bonds and C_∞ the characteristics ratio. The average of the reported C_∞ values for PVA is 8.3[25]. The equation then reduces to

$$DR_{min} = 0.41 DP^{1/2}$$

Calculations were made for $DP = 3500$, 7700 and 18 200 and the results are shown in *Table 1*. Also included in *Table 1* are the *MW* of PVA and the PE *MW* corresponding to the same chain length as the PVA. As cited above, the DR_{max} achieved here were ≈ 20 for all the *DP* used. DR_{max} is close to DR_{min} for $DP = 3500$, but significantly lower than those for the higher *DP* samples.

Table 1 *DP* and *MW* of PVA samples, the corresponding *MW* of PE (Red. PE *MW*) with the same chain length as the PVA, critical concentrations C^* and C_e, and DR_{min}

DP	PVA *MW*	Red. PE *MW*	C^* (%)	C_e (%)	DR_{min}
3500	154 000	98 000	0.45	5	24
7700	338 800	215 600	0.28	4	36
18 200	800 800	509 000	0.15	2	55

Berghmans *et al.*[26] have extensively studied the gelation behaviour of a PVA/EG system over a wide range of concentration (0.5–90 wt%). They report that phase separation is affected in a complex way by solution concentration, temperature and sample *DP*. On cooling the concentrated solutions, a liquid–liquid phase separation occurred rapidly, followed by crystallization in the resultant more concentrated phase. However, when the solution concentration and *DP* were decreased, the crystallization from solution preceded the liquid–liquid demixing. Indeed, we have also observed a similar phenomenon for crystallization at constant temperatures of 50–110°C. When a flask containing a hot 0.1 wt% solution of PVA with DP of 7700 in EG was transferred into a silicone oil bath at 110°C, the solution became cloudy due to the formation of small liquid particles. On standing the suspension at this temperature, the particle size increased with time by coagulation, and was followed by sedimentation due to crystallization, which increased the particle density. Our visual observations suggested that such a liquid–liquid phase separation might be partially suppressed when a hot solution was rapidly quenched at a lower temperature of 50°C, where the crystal nucleation and growth rates became reasonably fast compared to the liquid–liquid demixing. As will be detailed later, the SAXS patterns of the sedimented mats showed a broad long period scattering corresponding to a periodicity of 6.6 nm, indicating a lamellar nature of

the crystalline precipitates. The electron micrographs showed that the morphology of crystals precipitated under the present conditions was less regular than that of the typical single crystals grown from a dilute solution in triethylene glycol[27]. Further, the differential scanning calorimetry (d.s.c.) heats of fusion of these SGC mats showed a crystallinity of 60 wt%. These results indicate that a substantial amount of disorder was introduced during precipitation even from the dilute solutions.

Another important factor controlling the ductility of PVA is probably the strong intermolecular interaction due to hydrogen bonds[17], which may act as net points in both amorphous and crystalline regions, and reduces the ability of chain slippage and unravelling of crystalline lamellae. This may also increase the draw stress (*Figure 1*) and lower the ductility. The fact that the DR_{max} achieved was ≈ 20 for all *DP* samples suggests that this factor is probably more important in the present SGC samples.

Tensile properties

Figure 2 shows tensile modulus as a function of *DR* for drawing SGC mats of PVA with different *DP*. The moduli previously observed for drawing of SGC mats of UHMW-PE ($MW = 2.1 \times 10^6$) and normal MW-PE ($MW = 2 \times 10^5$)[14] are also included for comparison. The modulus of PVA increases rapidly with *DR* and reaches 50 GPa at the highest *DR* of 20. Independent of the *DP*, the moduli lie on a single curve. Such an increase in the modulus is significantly different from that observed in PE. As shown in *Figure 2*, the modulus of PE increases slowly in the lower *DR* region ($DR \leqslant 10$) and more rapidly at higher *DR* ($DR \geqslant 10$). Further, the moduli at the same *DR* are markedly higher for PVA than for PE, the higher *MW* PE having slightly higher moduli. In view of the comparable X-ray crystal moduli for PVA (250 GPa)[16] and PE (235 GPa)[16], this difference may be related to the differences in the glass transition temperature (T_g), the efficiency of draw in achieving the molecular extension and orientation and/or the supermolecular structure. The test temperature of ≈ 25°C in this work is far above the T_g of PE (−120 or −80°C) and below that of PVA (70°C). However, in highly crystalline linear PE, the modulus decrease at the T_g is small[7] and not enough fully to explain the difference. Thus, the lower modulus of PE should also be related to the latter factors. These will be discussed later based on the measurements of X-ray diffraction, d.s.c. and thermal elastic shrinkage.

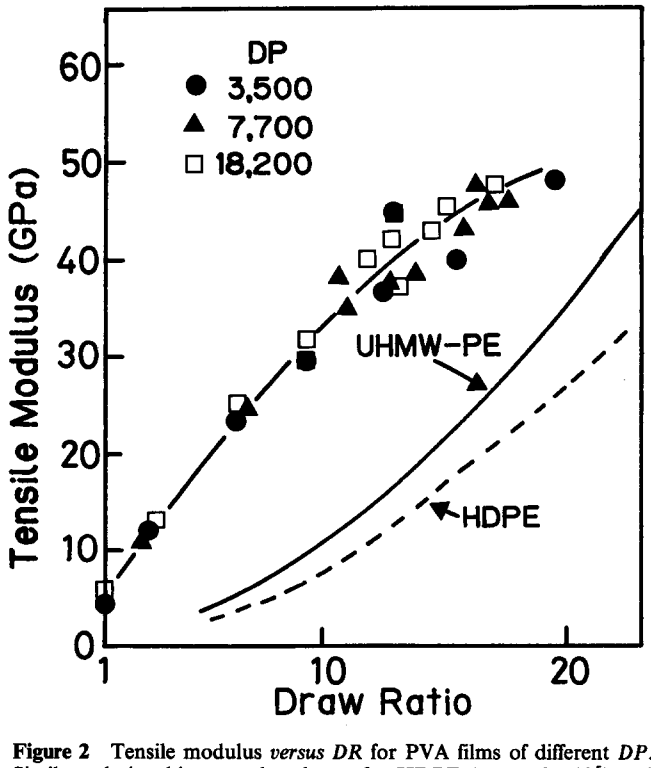

Figure 2 Tensile modulus *versus DR* for PVA films of different *DP*. Similar relationships are also shown for HDPE ($MW = 2 \times 10^5$) and UHMW-PE ($MW = 2.1 \times 10^6$)

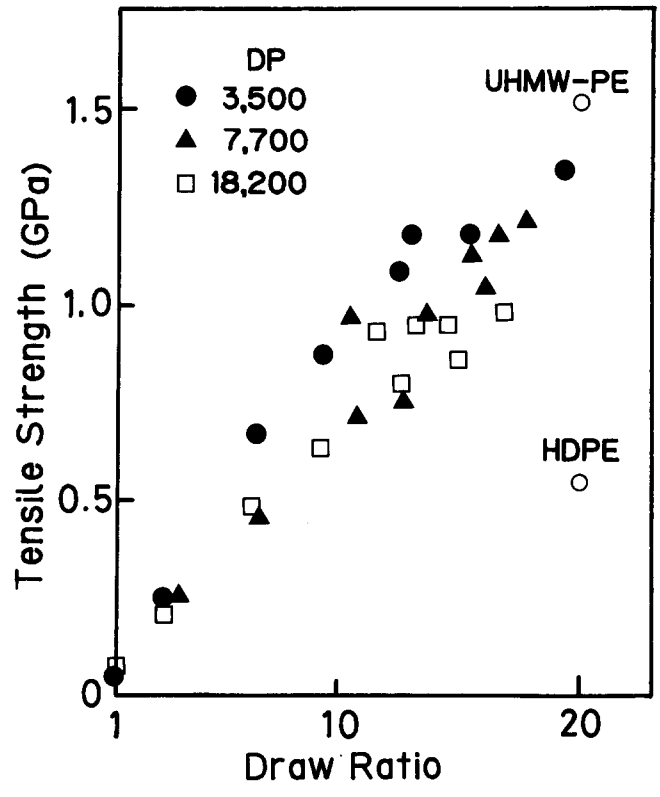

Figure 3 Tensile strength *versus DR* for PVA films of different *DP*. The strength of polyethylenes HDPE and UHMW-PE at $DR = 20$ are also included for comparison

Figure 3 shows tensile strength as a function of *DR*. The strength data at $DR = 20$ for drawn SGC mats of PE are also included. Again, the strength of PVA increases steadily with *DR* and reaches 1.3 GPa at $DR_{max} = 20$. This strength at $DR = 20$ is comparable to that for UHMW-PE but about twice that for the normal MW-PE with a chain length comparable to the PVA with $DP = 7700$ (see *Table 1*). Although the effect of *DP* on strength for drawn PVA films is not clear due to the wide scatter of data, there is a trend that lower *DP* samples have slightly higher strength. This results from the comparable modulus (*Figure 2*) but slightly larger strain at break for lower *DP* samples. Such an effect of *DP* is in sharp contrast to that observed in drawing SGC mats of PE with a wide range of *MW*, 2×10^5–80×10^5 [14]. In PE, the tensile strength at a given *DR*, as well as at the maximum achieved *DR*, increased dramatically with sample *MW*. Smith *et al.*[28] explained the effect of *MW* on the tensile strength of PE on the basis of theoretical calculation. The predominant mechanism of fracture for oriented PE changes from chain slippage for lower *MW* to bond rupture for higher *MW*. In contrast, PVA

has intermolecular hydrogen bonds depending on the tacticity[17]. This may suppress the chain slippage in oriented morphologies, resulting in a negligible effect of sample *DP* on room temperature tensile strength for the *DP* range studied. Such an explanation is consistent with the comparable strength for PVA and UHMW-PE at $DR=20$, and also with the more recent prediction by Smith *et al.*[3] of the *MW* effect on the strength of poly(*p*-phenylene terephthal amide) having hydrogen bonds.

As described above, the fracture stress measured at room temperature was almost independent of the *DP*, whereas that at the drawing temperature (220°C) was significantly higher for higher *DP* samples. This is probably related in part to the effect of temperature on the fracture mechanism, as discussed above in relation to PE[28]. At 220°C, the molecular motions in both amorphous and crystalline regions are highly activated[29]. Thus the intermolecular chain slippage may be much easier than at room temperature, resulting in the process being a more enhanced mechanism of fracture for lower *DP* samples at elevated temperatures.

The maximum tensile modulus and strength observed in this work for drawing PVA films are higher than those reported by Grubb *et al.*[18,19], but significantly lower than those achieved for drawing fibres by other workers[20,21,30]. In view of the fact that these reported tensile properties are independent of the *DR* and *DP* of samples, the properties are probably related to the detailed morphologies of drawn materials prepared by the different techniques and under the different conditions. Note, however, that the maximum tensile properties achieved are significantly lower for drawn films than for fibres. Ito *et al.*[31] report a similar effect of the sample size and shape on the maximum attainable *DR* and tensile properties in drawing of poly(ethylene terephthalate). These factors are probably another possible reason for the higher tensile properties achieved for fibres than for films.

X-ray diffraction

Figure 4 shows WAXD (top) and SAXS (bottom) patterns of the SGC mat and drawn films with $DR=$ 6–24.6. The sample with $DR=24.6$ was prepared by increasing the draw temperature up to 230°C during the second-stage drawing. These patterns of the SGC mat were recorded with the incident beam parallel to the wide surface of the mat. The patterns show that the molecular chains are almost randomly oriented and the lamellae 6.6 nm thick are partially oriented parallel to the mat surface. These facts indicate a slight chain inclination within a lamella. On drawing the mat, the chain orientation proceeded rapidly along the draw direction, as shown by a series of WAXD patterns. The SAXS patterns of an EDR 6 extrudate prepared at 160°C show a strong long period scattering (10 nm) on the meridian, extended perpendicular to the fibre axis. This indicates that the initial lamellar-like morphology has transformed to the fibrillar structure at EDR = 6. On further drawing the extrudate by tensile force at 220°C, the long period increased to 15.1 nm at $DR=12.5$ due to annealing. The scattering intensity decreased with increasing *DR*. At $DR=24.6$, strong void scatterings appeared around the direct beam and on the equator, but the long period scattering became negligibly weak even for a longer exposure time ($\approx$60 h) with a longer sample to film distance (400 nm). Such a decrease in intensity with increasing *DR* has been reported on drawing PE. The critical *DR*, above which the intensity of long period scattering approaches zero, has been found to be 50[32]–80[33] for drawing of SGC mats of UHMW-PE, depending on the drawing conditions and techniques used. The corresponding *DR* for PVA was $\approx$25, as found in this work. Although the SAXS intensity depends on several structural parameters, such a *DR* may be understood as the *DR* above which the initial amorphous-crystalline two-phase structure approaches a one-phase structure, in which the defects including the residual folds,

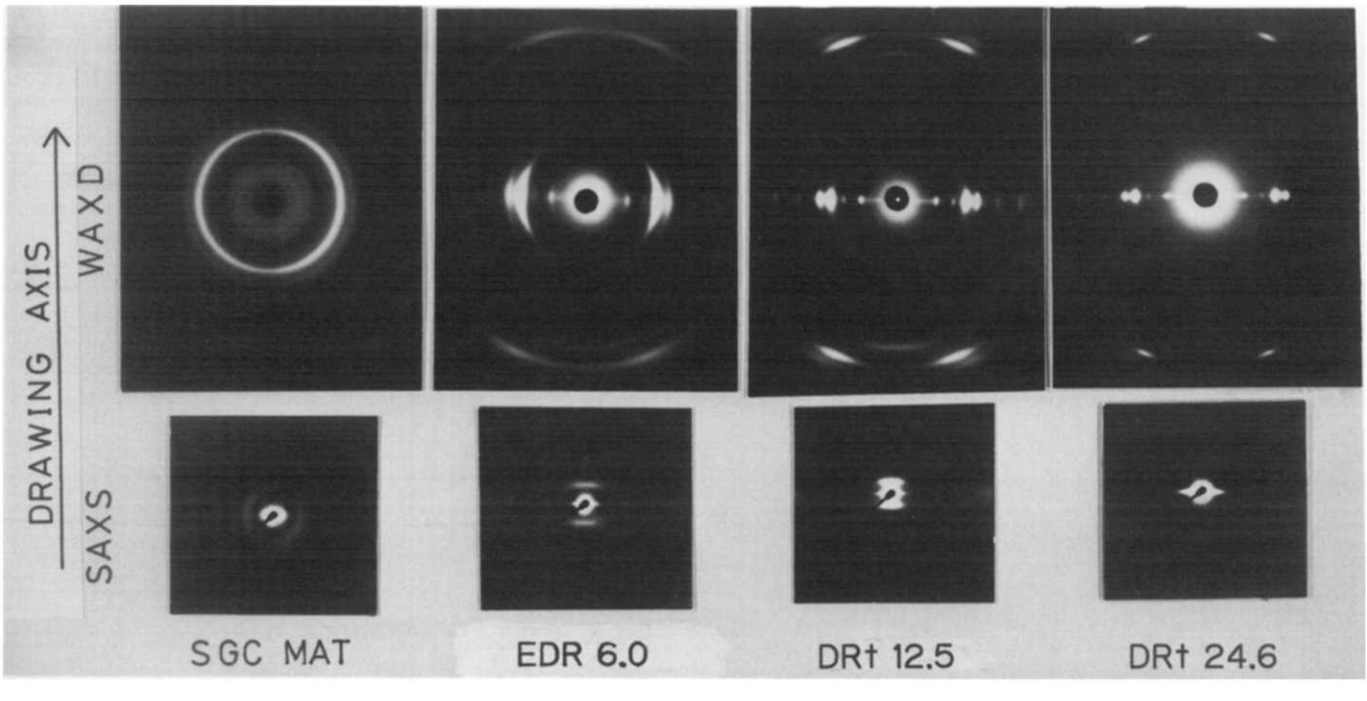

Figure 4 WAXD and SAXS patterns of an initial SGC mat and drawn films. The patterns of a mat were obtained with the incident beam parallel to the mat surface, which is perpendicular in the present mounting

trapped entanglements, chain ends etc. are distributed more or less randomly. Thus the fact that the critical *DR* for PVA is remarkably small compared with that for PE suggests a significantly higher efficiency of draw for the former polymer. The significantly higher moduli for PVA than for PE at the same *DR* in *Figure 2* may be primarily due to the higher efficiency of draw in PVA.

Closer inspection of the SAXS patterns in *Figure 4* revealed a weak but sharp and circular scattering on the meridian, which corresponds to a spacing of 4.2 nm. This reflection was observed on the photographs at $DR=6$ and 12.5 but not for the initial mat and a highly drawn film with $DR=24.6$. The shape and spacing of the reflection indicate that this is not a higher order reflection of the long period scattering. A similar reflection was observed for a commercial PVA fibre which was surface treated with a low *MW* compound. However, our samples were not treated with such a material. The origin of this feature is not clear at present and will be studied in the future.

Elastic shrinkage

It has been shown that thermally induced elastic shrinkage can be a sensitive measure for the efficiency of draw[3,34,35]. The correlations between this property in oriented polymers and tensile modulus[34,35], morphology[36] and chain extension determined by small-angle neutron scattering[37,38] have been discussed.

When a drawn PVA specimen was immersed and freely floated in silicone oil kept at a constant temperature above the melting point of PVA (≈240°C), elastic shrinkage quickly occurred and was completed in a few seconds. The percentage recovery for a given sample measured after 15 s was not affected by the temperature in the range 250–270°C and was 90–97% depending on the *DR*. The shrinkage was evaluated in terms of the molecular draw ratio (*MDR*)[34,35] defined by

$$MDR=(L_t-L_s)/L_0+1$$

where L_0 is the sample length before drawing, L_t the total length after drawing, and L_s the shrunk length after elastic recovery. The average values of four measurements at 270°C for each specimen were used. *Figure 5* shows *MDR* as a function of *DR* for PVA samples with different *DP*. Independent of *DR* and *DP*, the *MDR* are close to the macroscopic deformation ratio. Thus the efficiency of draw evaluated by the ratio of *MDR* to *DR* was high and in the range 0.94–0.97 for each drawn specimen. The result indicates that the sample *DP* actually had no effect on the efficiency of draw in achieving the molecular extension. Recently, Shibayama *et al.*[38] reached a similar conclusion: that each PVA molecule was deformed to the same extent as the macroscopic sample *DR* based on the small angle neutron scattering study of drawn PVA with a lower *DP* of 1800.

D.s.c. melting behaviour

The effects of *DR* and *DP* on the melting behaviour of PVA have been studied by d.s.c. *Figure 6* shows two series of thermograms observed on the lowest (3500) and the highest (18 200) *DP* samples used in this study. For each *DP*, the initial SGC mat showed a fairly broad, single melting peak. With increasing *DR*, the peak became sharper and shifted to higher temperatures. As shown in *Figure 7*, the melting peak temperature

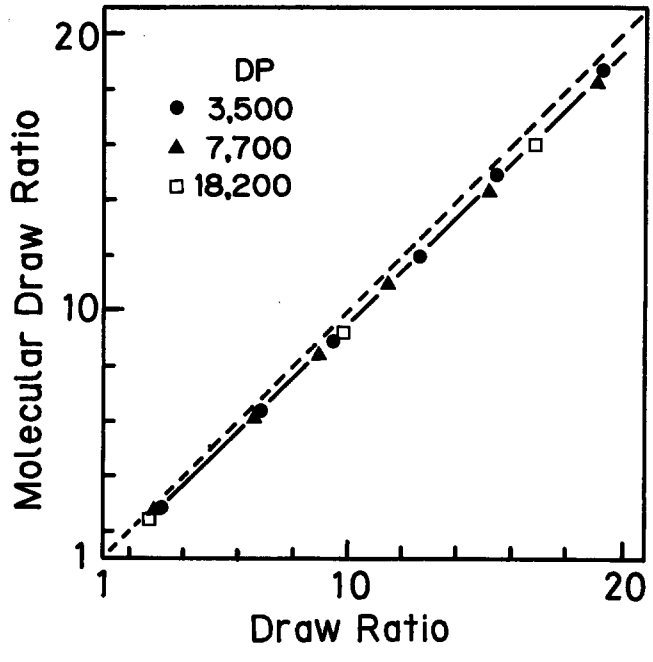

Figure 5 Molecular *DR versus* macroscopic *DR* for samples of different *DP*. The dotted line represents perfect efficiency of draw ($DR=MDR$)

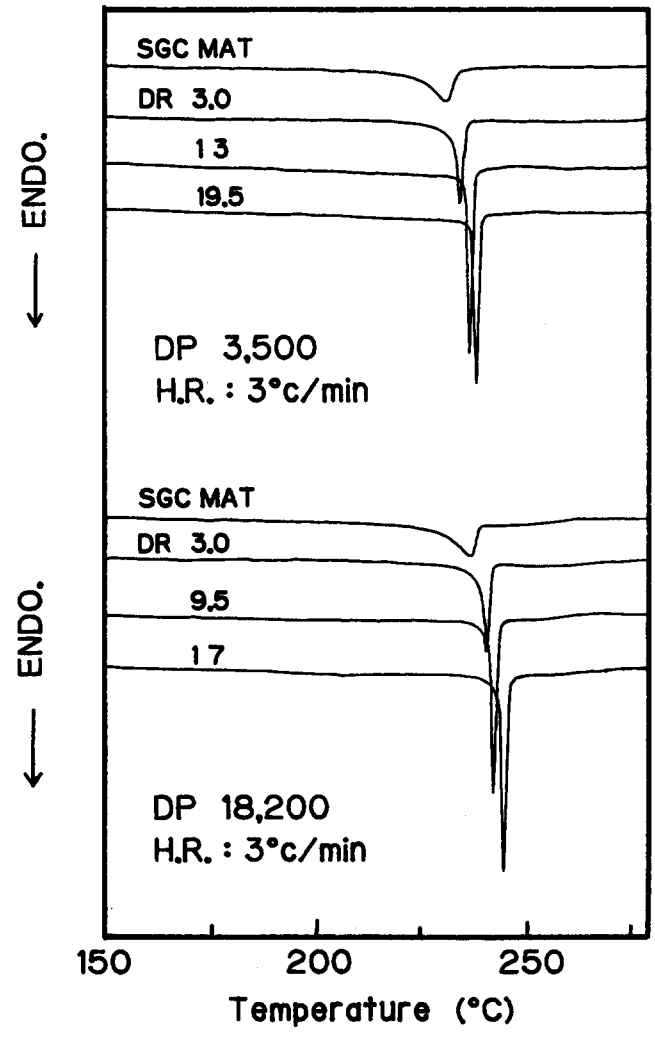

Figure 6 D.s.c. thermograms of SGC mats and drawn films prepared from PVA with $DP=3500$ (upper) and 18 200 (lower). Heating rate was 3°C min^{-1}

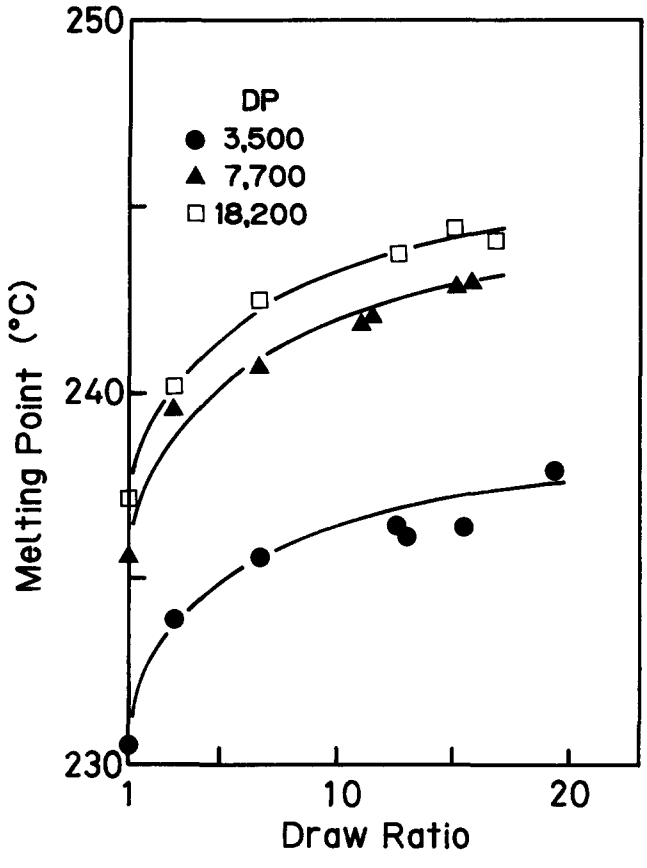

Figure 7 D.s.c. melting peak temperature *versus DR* for samples of different *DP*

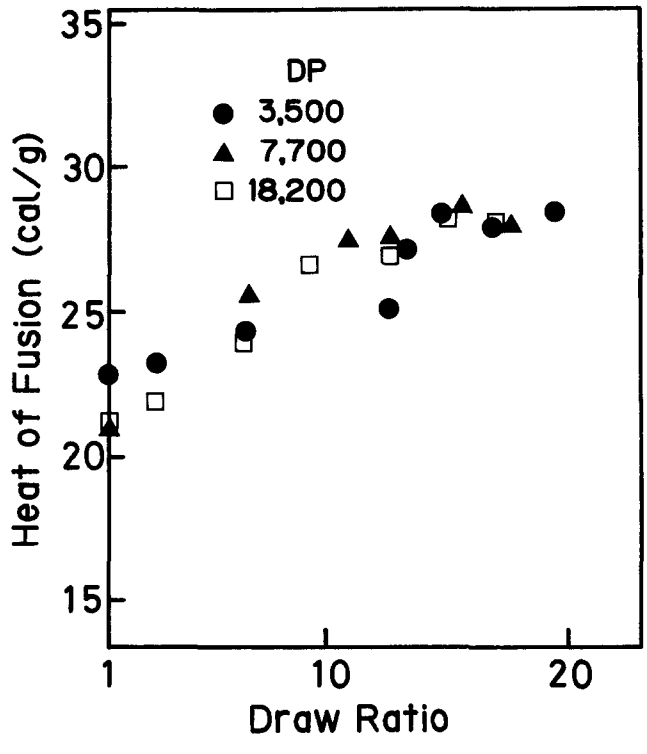

Figure 8 Heat of fusion *versus DR* for samples of different *DP*

increased rapidly with *DR* in the lower *DR* range (<10) and slowly at higher *DR* (>10). This effect of *DR* on melting behaviour has often been observed in the drawing of other polymers[1]. The melting temperature at a given *DR* was markedly higher for a higher *DP*, showing the significant effect of *DP* on the d.s.c. melting behaviour of drawn PVA. This is primarily due to enhanced superheating for higher *DP* samples. *Figure 8* shows heat of fusion as a function of *DR* for three sample *DP*. The heat of fusion for the initial SGC mats was 21.5–23 cal g^{-1} for all *DP*, corresponding to a crystallinity of 60 wt%, taking the heat of fusion of a perfect PVA crystal as 37.5 cal g^{-1} [17]. For all *DP* samples, heats of fusion lie on a single curve, increase rapidly with *DR* in the lower *DR* range ($DR<15$) and approach a constant value of 28.5 cal g^{-1} at higher *DR*, which corresponds to a crystallinity of 76 wt%.

CONCLUSION

SGC mats of PVA with *DP* from 3500 to 18 200, grown from dilute solutions in EG, have been drawn by solid state coextrusion at low *DR* of 3–6, followed by tensile drawing at 220°C (two-stage drawing). The effect of sample *DP* on drawing of PVA has been studied and the results compared with those previously observed on drawing SGC mats of PE with wide range of molecular weights. The *DP* of PVA had a marked effect on the drawing and fracture stresses during the second-stage tensile drawing at elevated temperatures and on d.s.c. melting peak temperatures measured as a function of *DR*; these properties were significantly higher for the higher *DP* samples. However, *DP* had no important effect on the maximum achieved *DR*, the tensile modulus and strength and the crystallinity measured as a function of *DR*. The latter results for PVA are markedly different from those previously observed in drawing SGC mats of PE with a wide range of *MW*. Possible explanations have been proposed for the differences observed between PVA and PE. However, as the ductility of a polymer in general is known to be affected in a complex way by several factors including the initial morphology, *MW* and drawing technique, the effects of these variables are currently under study.

REFERENCES

1 Zachariades, A. E. and Porter, R. S. (Eds) 'Strength and Stiffness of Polymers', Plastic Engineering Series, Vol. 4, Marcel Dekker, New York, 1983
2 Barham, P. J. and Keller, A. *J. Mater. Sci.* 1985, **20**, 2281
3 Zachariades, A. E. and Porter, R. S. (Eds) 'High Modulus Polymers', Plastic Engineering Series, Vol. 17, Marcel Dekker, New York, 1988
4 Zwijnemberg, A. and Pennings, A. *Colloid Polym. Sci.* 1976, **254**, 868
5 Smith, P. and Lemstra, P. J. *Polymer* 1980, **21**, 1341
6 Matsuo, M. and Sawatari, C. *Macromolecules* 1986, **19**, 2036
7 Roy, S. K., Kyu, T. and Manly, R. St. J. *Macromolecules* 1988, **21**, 1746
8 Furuhata, K., Yokokawa, T. and Miyasaka, K. *J. Polym. Sci., Polym. Phys. Edn* 1984, **22**, 133
9 Kunugi, T., Oomori, S. and Mikami, S. *Polymer* 1988, **29**, 814
10 Smith, P., Lemstra, P. J. and Booij, H. C. *J. Polym. Sci., Polym. Phys. Edn* 1981, **19**, 877
11 Lemstra, P. J., Van Aerle, N. A. J. M. and Bastiaansen, C. W. N. *Polym. J.* 1987, **19**, 85
12 Kanamoto, T., Tsuruta, A., Tanaka, K., Takeda, M. and Porter, R. S. *Polymer J.* 1983, **15**, 327
13 Kanamoto, T., Tsuruta, A., Tanaka, K., Takeda, M. and Porter, R. S. *Macromolecules* 1988, **21**, 470
14 Kanamoto, T. and Porter, R. S. 'Integration of Fundamental Polymer Science and Technology' (Eds P. J. Lemstra and L. A. Kleintjens), Elsevier Applied Science, London, Vol. 3, 1989, p. 168

15 Griswold, P. D., Zachariades, A. E. and Porter, R. S. *Polym. Eng. Sci.* 1978, **18**, 861
16 Sakurada, I., Ito, T. and Nakamae, K. *J. Polym. Sci. C*, 1966, **15**, 75
17 Sakurada, I. 'Polyvinyl Alcohol Fibers', Marcel Dekker, New York, 1985
18 Cebe, P. and Grubb, D. *J. Mater. Sci.* 1985, **20**, 4465
19 Garrett, P. D. and Grubb, D. *Polym. Commun.* 1988, **29**, 60
20 Kwon, Y. D., Kavesh, S. and Prevorsek, D. C. US Patent no. 4440711, 1984
21 Hyon, S. H., Cha, W. I. and Ikada, Y. Sen-i Gakkai Symp. Preprints (Japan), 1987, p. 34
22 Narukawa, H. Workshop on Polymer Solutions (SPSJ), Tokyo, Preprints, 13, May 26, 1989
23 Sanefuji, T., Narukawa, H., Kajitani, K. and Monobe, K. *Polym. J.* submitted for publication
24 Kanamoto, T. and Porter, R. S. *J. Polym. Sci., Polym. Lett. Edn.* 1983, **21**, 1005
25 Brandrup, J. and Immergut, E. H. (Eds) 'Polymer Handbook', Wiley, New York, 1974
26 Stoks, W., Berghmans, H., Moldenaes, P. and Mewis, J. *Br. Polym. J.* 1988, **20**, 361
27 Monobe, K. and Fujiwara, Y. *Kobonshi Ronbunshu* 1964, **21**, 179
28 Termonia, Y., Meakin, P. and Smith, P. *Macromolecules* 1985, **18**, 2246
29 Garrett, P. D. and Grubb, A. T. *J. Polym. Sci., Polym. Phys. Edn.* 1988, **26**, 2509
30 Fujiwara, H., Shibayama, M., Chien, J. H. and Nomura, S. *J. Appl. Polym. Sci.* 1989, **37**, 1403
31 Ito, M., Takahashi, K. and Kanamoto, T. *Polymer* 1990, **31**, 58
32 Kanamoto, T. unpublished data
33 Furuhata, K., Yokokawa, T., Seoul, C. and Miyasaka, K. *J. Polym. Sci., Polym. Phys. Edn.* 1986, **24**, 59
34 Watts, M. P. C., Zachariades, A. E. and Porter, R. S. *J. Mater. Sci.* 1980, **15**, 426
35 Porter, R. S., Daniels, M., Watts, M. P. P. C. and Zachariades, A. E. *J. Mater. Sci.* 1981, **16**, 1134
36 Barham, P. J. and Keller, A. *J. Polym. Sci., Polym. Lett. Edn.* 1975, **13**, 197
37 Hadziioannou, G., Wang, L. H., Stein, R. S. and Porter, R. S. *Macromolecules* 1982, **15**, 880
38 Shibayama, M., Kurokawa, H., Nomura, S., Roy, S., Stein, R. S. and Wu, W. *Polym. Prepr. Jpn* 1989, **38**, 875; *Macromolecules* 1990, **23**, 1438